GEOPHYSICAL RESEARCH, 2020, vol. 21, no. 3, pp. 5-18. https://doi.org/10.21455/gr2020.3-1

UDC 550.34.01

PRELIMINARY RESULTS OF THE ATMOSPHERIC GRAVIMETRIC EFFECT CALCULATIONS

E.A. Spiridonov, O.Yu. Vinogradova

Schmidt Institute of Physics of the Earth, Russian Academy of Sciences, Moscow, Russia

Abstract. Preliminary results of calculation of the atmospheric gravimetric effect for 2006 are presented. The calculation was based on the spherical expansion of the surface atmospheric pressure fields of the European reanalysis project *ERA*5, according to the method described in [*Spiridonov,* 2019]. This technique involves the calculation of the sum of the atmospheric loading effect and direct Newtonian attraction created by the air masses.

Comparison of the calculated time series of the effect with observational data on six superconducting gravimeters of the Global Geodynamic Project (GGP) network located in *Bad Homburg, Medicina, Membach, Moxa, Strasbourg* and *Vienna*, as well as with the series taken from the *EOST* website was carried out.

To remove the tide in the inelastic rotating self-gravitating Earth with the ocean from the series of observations the program ATLANTIDA3.1_2017 was used [*Spiridonov et al.,* 2017]. The amplitude delta-factors of tidal waves for this program were calculated in [*Spiridonov,* 2017], and the loading delta-factors used in the calculation of the ocean load effect are shown in [*Spiridonov, Vinogradova,* 2017]. To calculate the oceanic gravimetric effect the oceanic tidal model FES2012 was applied.

The analysis of the results of calculating the atmospheric gravimetric effect obtained both with and without taking into account the inverted barometer effect is carried out.

The standard deviations of the difference series obtained by subtracting from the series of observations the dynamic tide, the ocean effect, and the atmospheric effect calculated in this work do not exceed 0.2–0.3 μGal in the period range from 4 to 60 days.

Keywords: Earth's tides, atmospheric gravimetric effect, atmospheric gravitational attraction, atmospheric loading effect.

Introduction

The purpose of this article is a preliminary assessment of the quality of the atmospheric gravimetric effect calculation results, performed according to the method described in [*Spiridonov,* 2019]. This method provides the calculation of both the atmospheric loading effect and the Newtonian direct attraction created by air masses using in both cases the simple spherical layer method. To calculate the atmospheric gravimetric effect, the spherical harmonic expansion of the surface atmospheric pressure of the European reanalysis *ERA5* project was used, rather than Green's functions that are used in almost all similar works of other researchers. This approach significantly reduces the time and volume of calculations, while excluding the need to introduce near and far zones, which makes it possible to determine the gravimetric effect of the atmosphere at a given point at a given time, taking into account at once all the features of the atmosphere behavior on the entire Earth's surface, and not on its predetermined ones.

The quality of the calculation results was assessed by comparing the calculated time series of the atmospheric gravimetric effect with the observational data carried out by modern superconducting gravimeters at six stations of the *GGP* network located in Europe (Fig. 1). The main characteristics of the series of gravimetric observations at these stations are presented below right after a brief description of the *ERA5* surface pressure data and the specifics of calculating the atmospheric effect.

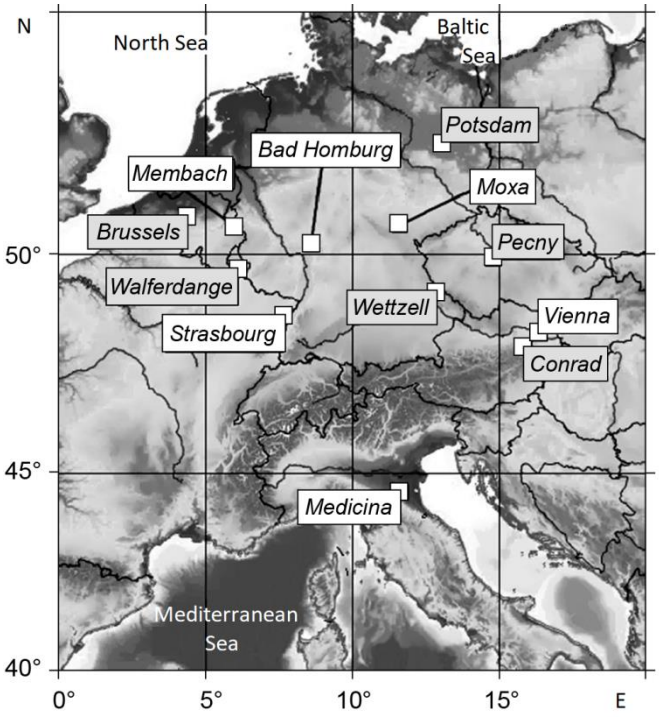

Fig. 1. The *GGP* network gravity observation points in Europe. The names of the points whose observations are used in this article are given in rectangles without filling

To obtain the experimental curve of the atmospheric gravimetric effect, the theoretical tide calculated for the elastic rotating Earth with the ocean should be subtracted from the observations. This is also discussed in this article.

The series of the atmospheric gravimetric effect calculated in this work are compared with the series obtained by other authors. Besides, a detailed comparative analysis of the degree of closeness of different calculated variants to the observed series was also carried out.

The last section of the work is devoted to the software implementation of the calculations performed during its preparation; a brief description of the program AURORA1.0_2019 for calculating the atmospheric gravimetric effect is given.

Initial data and calculation methods

To calculate the atmospheric gravimetric effect, the authors applied the spherical harmonic expansions of surface atmospheric pressure maps at mesh points 0.25×0.25° with a time step of 1 hour. These data, which are freely available at https://cds.climate.copernicus.eu/, are obtained in the framework of the latest *ERA5* global atmospheric reanalysis project by the European Center for Medium-Range Weather Forecasts (*ECMWF*) [*Dee*, 2011]. The expansion of the surface pressure was carried out up to 360 order; 8,760 hourly data files for 2006 were processed.

Newtonian (Δg_{direct}) and load (Δg_{load}) components of the effect were calculated by the formulas

$$\Delta g_{\text{direct}} = -\frac{3}{\rho_0 a}\sum_{n=0}^{\infty}\frac{n}{2n+1}\sum_{k=0}^{n}\left(A_n^k\cos(k\lambda)+B_n^k\sin(k\lambda)\right)\cdot P_n^k\,,$$

$$\Delta g_{\text{load}} = -\frac{6}{\rho_0 a}\sum_{n=0}^{\infty}\frac{\delta_n}{2n+1}\sum_{k=0}^{n}\left(A_n^k\cos(k\lambda)+B_n^k\sin(k\lambda)\right)\cdot P_n^k\,,$$

where ρ_0 and a – average density and average radius of the Earth; n – the order of spherical harmonic expansion of atmospheric pressure; A_n^k and B_n^k – the coefficients of this expansion;

P_n^k – Legendre polynomials of order *n* and degree *k* (see formulas (6), (7) in [*Spiridonov*, 2019]).

Two variants of calculations were analyzed - with and without taking into account the inverse barometer effect. In the second case, the "land – ocean" mask was applied, recalculated into mesh points 0.25×0.25°. That helped to reset to zero the values of the surface atmospheric pressure over the ocean surface.

In [*Spiridonov*, 2019], the total series of the atmospheric gravimetric effect was considered as the sum of four series - the atmospheric loading effect, the attraction of the atmosphere, and corrections to these two series for the finiteness of the expansion order.

Below, as an example, the plots of the atmospheric loading effect and atmospheric attraction of 2006 for *Vienna* station are presented (Fig. 2). Previously, their average values were removed from the series.

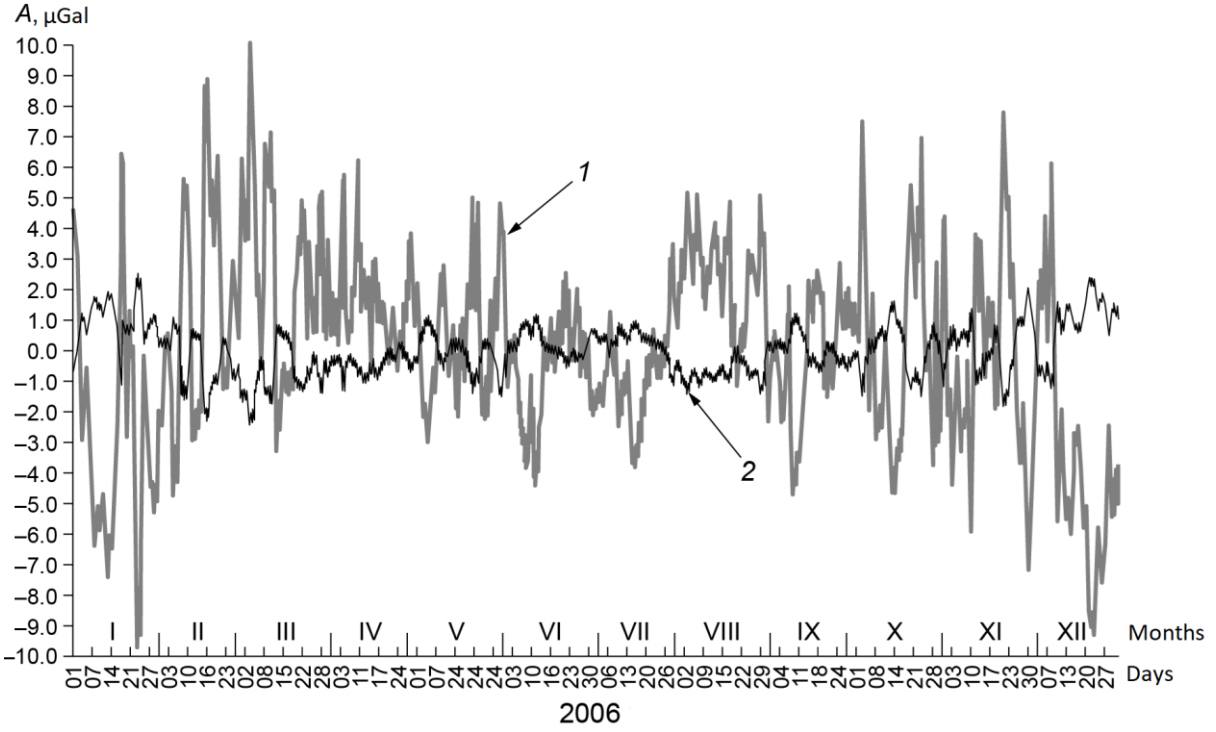

Fig. 2. Plots of atmospheric attraction (curve *1*) and atmospheric loading effect (curve *2*) in *Vienna* point of the *GGP* network. Observations of 2006

As can be seen in Fig. 2, the attraction of the atmosphere is several times greater than the loading effect. So, if the amplitude of the loading effect usually does not exceed 2–3 μGal, then the attraction of the atmosphere can reach 10 μGal. The RMSD values for the series of attraction are 3.086 μGal, for the series of the loading effect – 0.815 μGal.

In addition to the four components of the atmospheric gravimetric effect, considered earlier in [*Spiridonov*, 2019], in this work, the authors took into account the fifth component - the time-varying atmospheric loading effect. This effect is associated with changes in the average surface atmospheric pressure, which are caused by variations in the mass of the atmosphere due to fluctuations in its humidity. It can be calculated by the formula $\Delta g_{\text{load}}^0 = -\frac{6h'_0}{\rho_0 a} C_0^0$, where $\rho_0 = 5.5134 \cdot 10^3$ kg/m^3 – the average value of the Earth's density; *a* – the average radius of the Earth; $h'_0 = -0.1326$ – the zero-order load Love number [*Spiridonov*,

Vinogradova, 2017]; $C_0^0 = \overline{p} = \frac{1}{4\pi}\int p(\theta,\lambda)d\sigma$, – the average over the earth's surface (land + ocean) surface atmospheric pressure $\overline{p}$, where $p(\theta, \lambda)$ is the surface atmospheric pressure, which is a function of colatitude θ and longitude λ; $d\sigma = \sin\theta d\theta d\lambda$ – surface element of a sphere of unit radius. The amplitude of the effect is about 0.035 μGal; the overwhelming part of the dispersion of the series falls on *Sa* annual wave. This effect is calculated without taking into account the inverse barometer effect, which does not work for the average pressure.

The results obtained by the authors were compared with the results of other researchers, in particular, with the series of the atmospheric gravimetric effect published on the *EOST*[1] website, calculated using the Green's functions plotted for the entire surface of the globe with the selection of the near zone. The method for calculating these series is described in [*Boy, Gegout, Hinderer,* 2002; *Boy, Chao,* 2005; *Boy, Hinderer,* 2006], which are a continuation of the already classic articles [*Warburton, Goodkind,* 1977; *Spratt,* 1982; *Merriam,* 1992].

As noted above, the quality of the gravimetric atmospheric effect calculation was also evaluated by comparing the obtained results with observational data at six European points of the *GGP* network (see Fig. 1): *Bad Homburg*, *Medicina*, *Membach*, *Moxa*, *Strasbourg*, *Vienna*. The main characteristics of these points with an indication of the timing of observations on them are given in Table 1; the table also includes the values of the regression coefficients obtained from our data (k_S) and published on the *EOST* (k_{EOST}) website. In fact, these coefficients are multipliers designed to convert the series of atmospheric pressure into the series of atmospheric gravimetric corrections.

Modern superconducting gravimeters are characterized by an unprecedented (nanogal) resolution in a wide frequency band with a stability approaching several μGal / year. This ensures the most accurate measurement of long-term (from years to decades) gravitational signals, i.e. registration of a wide range of processes from long-period seismicity (1000 s) to tectonic movement of the earth's crust, occurring for many years or decades [*Hinderer, Crossley,* 2004].

Table 1. The main characteristics of the *GGP* network points, which observational data are used in this article

Points	Coordinates		Altitude	Tools	Period of observations		Regression coefficients, $nm \cdot s^{-2} \cdot GPa^{-1}$	
	θ, ° N	λ, ° E	*h*, m		Beginning	End	k_S	k_{EOST}
Bad Homburg	50.229	8.611	190	GWR 30_L + GWR C044	13.02.2001	30.01.2013	–3.373	–3.06679
Medicina	44.522	11.645	28	GWR C023	02.01.1998	30.01.2014	–3.559	–3.06679
Membach	50.609	6.007	250	GWR C021	04.08.1995	30.12.2011	–3.304	–3.06679
Moxa	50.646	11.616	455	CD 034 HIGH	02.01.2000	29.06.2012	–3.339	–3.06679
Strasbourg	48.622	7.684	185	GWR C026	02.03.1997	30.12.2012	–3.380	–3.06679
Vienna	48.249	16.357	193	SUP-GWR C025	02.08.1995	21.10.2007	–3.498	–2.21047

[1] *EOST – **E**cole et **O**bservatoire des **S**ciences de la **T**erre de l'Universite de Strasbourg* (School and Observatory of Earth Sciences of the University of Strasbourg). http://loading.u-strasbg.fr/surfg_form.php

To remove the tide in an inelastic rotating self-gravitating Earth with an ocean from the observation series ATLANTIDA3.1_2017 program was used [*Spiridonov et al.*, 2017]. The amplitude delta factors of tidal waves used by the program were calculated in [*Spiridonov*, 2017]; load delta factors used in calculating the oceanic loading effect are given in [*Spiridonov, Vinogradova*, 2017].

Comparison of the results of the atmospheric gravimetric effect calculation with observational data at the *GGP* network points

Not only the series of the atmospheric gravimetric effect calculated in this work (hereinafter referred to as "*S* series"), but also similar series published on the *EOST* website (hereinafter referred to as "*EOST* series") were compared with the observational data at the *GGP* network points. Therefore, it seems necessary and interesting to compare these series with each other. The statistical characteristics of the *S* and *EOST* series for six points of the *GGP* network are given in Table 2; calculations for both sets of series are performed taking into account the inverse barometer effect. The similarity of the series calculated by different methods can be judged from Fig. 3, which shows their comparison for *Vienna* point.

When comparing the *S* and *EOST* series, their similarity immediately attracts attention which is especially surprising, since significantly different methods were used in calculating the series. Our calculations (*S* series) are based on the spherical harmonic expansion of surface atmospheric pressure over a grid of the entire globe. When calculating the *EOST* series, Green's functions were applied in the near (up to 0.25° in latitude and longitude) and far zones. And although the calculations performed according to the named methods are mathematically completely identical, in practice, the obtained results can be significantly different from each other. In addition, the applied method does not involve data on changes in atmospheric pressure with altitude, since it was previously shown (see [*Spiridonov*, 2019]) that this does not lead to a noticeable increase in accuracy.

Table 2. Statistical characteristics of the series of atmospheric gravimetric effect for six points of the *GGP* network, obtained in this work (*S* series, in bold), and similar series published on the *EOST* website (*EOST* series)

Point	Series	Average value for the series	Root mean square deviation (RMSD)		
			For the series	For difference of ***S*** and *EOST* series	
		μGal	μGal	μGal	%
1	2	3	4	5	6
Bad Homburg	***S***	**–151.944**	**2.561**	0.093	3.6
	EOST	–0.145	2.553		
Medicina	***S***	**–163.175**	**2.317**	0.135	6.0
	EOST	–0.298	2.210		
Membach	***S***	**–155.586**	**2.717**	0.119	4.4
	EOST	–0.106	2.668		
Moxa	***S***	**–134.379**	**2.460**	0.133	5.5
	EOST	–0.195	2.415		
Strasbourg	***S***	**–151.223**	**2.353**	0.205	8.8
	EOST	–0.139	2.319		
Vienna	***S***	**–130.247**	**2.263**	0.196	8.6
	EOST	–0.267	2.278		

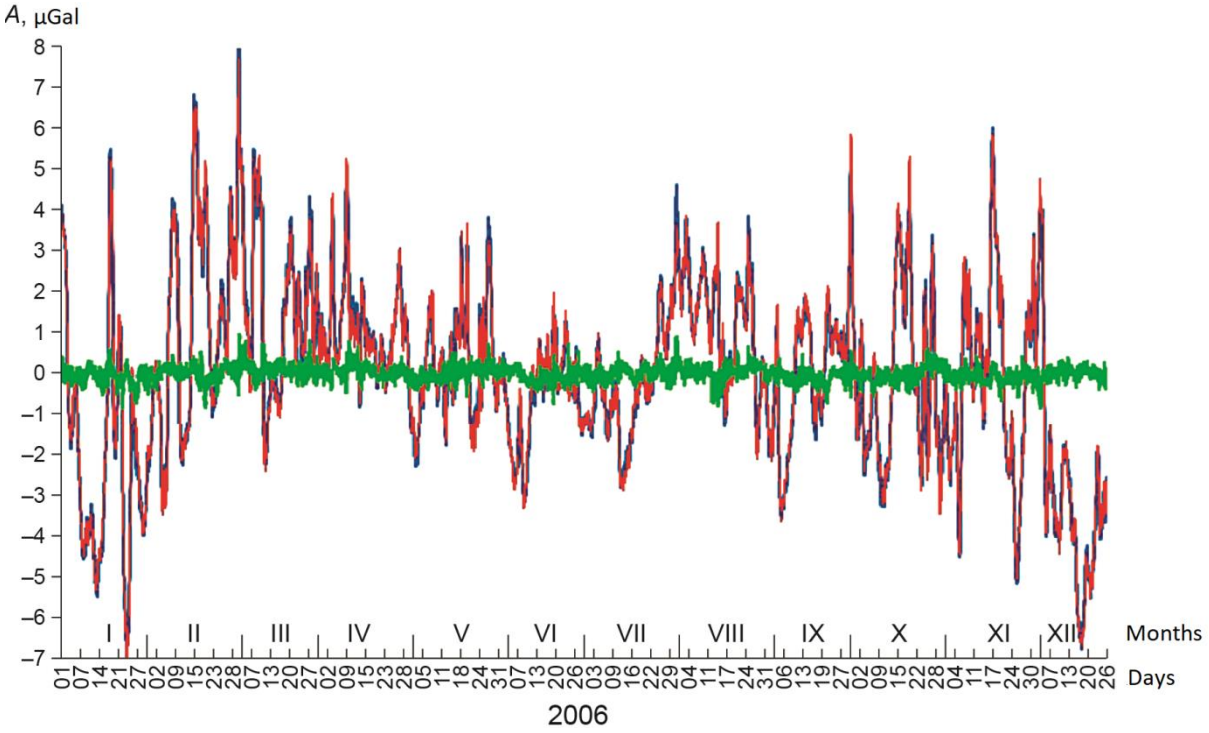

Fig. 3. Comparison of the series of atmospheric gravimetric effect calculated by the authors (*S* series, *red curve*) with the series published on the *EOST* website (*EOST* series, *blue curve*). The green curve is the difference between the *S* and *EOST* series. Observations of 2006, *Vienna* point of the *GGP* network

In the analysis of statistical characteristics given in Table 2, rather large average values for the *S* series (see column 3, bold type), lying in the range from –130.247 to –163.175 μGal, attract attention. The maximum difference of 32.928 μGal was noted between *Vienna* and *Medicina*; the minimum (0.721 μGal) - between *Strasbourg* and *Bad Homburg*. Such significant differences, firstly, can be caused by low-frequency trends that can be detected on large time scales; secondly, it is likely that some of these average values are a consequence of the atmospheric action at a given point, which can be considered constant in time. In the latter case, the same absolute gravimeter will invariably in time show different values of the gravitational acceleration at different points of the globe only due to the Newtonian attraction of the atmosphere, which basically sets large differences in average values.

This issue requires more detailed consideration on time series that are significantly longer than the annual one. So far, we can only additionally note that the obtained average values of the series do not correlate with height of the stations above sea level.

The smallest RMSD for the series of the atmospheric effect are observed at *Vienna* point (2.263 μGal for the *S* series and 2.278 μGal for the *EOST* series), the largest at *Membach* point (2.668 μGal for the *S* series and 2.717 μGal for the *EOST* series), i.e. the difference between observation points for this indicator can reach 0.4–0.45 μGal. The smallest RMSD value of the difference series obtained by subtracting the results published on the *EOST* website from our data (see Table 2, column 4) is observed at *Bad Homburg* (0.093 μGal or 3.6%), and the largest - at *Strasbourg* (0.205 μGal or 8.8%) and *Vienna* (0.196 μGal or 8.6%).

It is clear that such differences are significant in terms of accuracy of the modern gravimetric observations, and therefore it is advisable to see if any of the compared series – *S* or *EOST* – are closer in their values to observations at the GGP network points.

In addition, we must add that we did not carry out a comparison of series in terms of the spectral composition due to their limited length, but in the future, we expect to come back to this issue.

Further analysis can be carried out using Table 3, which presents the results of comparing the calculations performed for the six points of the *GGP* network considered in this work, as applied to different variants of the difference series. The results of calculations for the *S* series are highlighted in bold, without highlighting - for the *EOST* series.

In Table 3 and further in the text, when describing the variants of the difference series, the following notations are used:

OBS – observed series of gravimetric measurements at the considered points of the *GGP* network;

TH – TH – theoretical values of the dynamic tide in an inelastic rotating self-gravitating Earth with an ocean, calculated using the ATLANTIDA3.1_2017 program;

Patm – atmospheric gravimetric effect;

PM – correction for pole movement;

TREND – low frequency trend;

TIDE – residual tide in the range of periods up to 4 days.

One asterisk in the table marks the results of calculations taking into account the inverse barometer effect, two asterisks – without it.

Table 3. Root-mean-square deviations (RMS, μGal) for different variants of difference series, illustrating the comparison of theoretical series of the atmospheric gravimetric effect, calculated by the authors (series *S*, bold) and published on the *EOST* website (*EOST* series) with the series of gravimetric observations at six points of the *GGP* network

	Variant of difference series	*Bad Homburg*	*Medicina*	*Membach*	*Moxa*	*Strasbourg*	*Vienna*
1	*OBS –TH*	2.809	2.523	3.192	2.403	2.314	2.272
2		**1.475**	**1.554**	**1.384**	**1.048**	**1.147**	**0.770**
3	*OBS–TH–Patm*	**1.478**	**1.902**	**1.291**	**0.955**	**0.921**	**0.835**
4	*OBS–TH–Patm–PM*	1.449	1.436	1.385	0.950	1.117	0.769
5		1.490	1.772	1.261	0.829	0.875	0.695
6		**1.472****	**1.115****	**1.716****	**0.973****	**1.128****	**0.673****
7	*OBS–TH–Patm*	**1.470****	**1.559****	**1.550****	**0.784****	**0.903****	**0.539****
8	*OBS–TH–Patm–PM*	1.406*****	1.008*****	1.717*****	0.973*****	1.115*****	0.630*****
9		1.385*****	1.357*****	1.548*****	0.782*	0.866*	0.482*
10	*OBS–TH–Patm*	**1.427***	**1.029***	**1.745***	**0.959***	**1.111***	**0.608***
11	*OBS–TH–Patm–PM*	**1.406***	**1.403***	**1.563***	**0.762***	**0.882***	**0.434***
12	Δ1 (*OBS–TH–Patm)*	–0.021*****	–0.021*****	–0.028*****	0.014*	0.004*	0.022*
13	Δ2 (*OBS–TH–Patm–PM)*	–0.021*****	–0.046*****	–0.015*****	0.020*	–0.015*	0.048*
14	*TREND*	**1.356***	**1.359***	**1.405***	**0.657***	**0.758***	**0.365***
15		1.327*****	1.284*****	1.380*****	0.676*	0.772*	0.384*
16	*OBS–TH–Patm–PM–TREND–TIDE*	**0.296***	**0.291***	**0.342***	**0.334***	**0.264***	**0.226***
17		0.299*****	0.299*****	0.320*****	0.353*	0.296*	0.260*
18	Δ3(*OBS–TH–Patm–PM–TREND–TIDE*)	0.003*****	0.007*****	–0.022*****	0.019*	0.032*	0.035*

Note: * – calculations taking into account the inverse barometer effect (*IB*), ** - without it (*nonIB*).

Row 1 of Table 3 shows the results for the difference series obtained by subtracting of the theoretical values of the dynamic tide in an inelastic rotating self-gravitating Earth with an ocean (*TH*) from the observed series (*OBS*). The ATLANTIDA3.1_2017 program was used to calculate the theoretical values. The minimum (2.272 μGal) RMS deviation of the *OBS – TH* difference series was noted at *Vienna* point, the maximum (3.192 μGal) - at *Membach* point.

The calculations presented in rows 2–5 illustrate the effectiveness of the regression coefficients in calculating the atmospheric gravimetric effect (see Table 1 for the values of the regression coefficients). The results of the analysis carried out by the authors are highlighted in bold; results shown on the *EOST* website are given in regular type. In both cases, the upper rows (see rows 2, 4) present the RMSD values for the *OBS–TH–Patm* difference series, where *Patm* is the atmospheric gravimetric effect values calculated from the microbarograph readings using the corresponding regression coefficients; in the bottom rows - the values of the RMS deviations for the difference series *OBS–TH–Patm–PM*, where *PM* is the correction for pole movement (pole tide). First of all, we see that the subtraction of the atmospheric effect leads to a decrease in RMSD value of the OBS – TH difference series in two or more times. Additional subtracting of the pole tide reduces the RMS deviations at four points out of six - *Membach, Moxa, Strasbourg, Vienna*. At *Bad Homburg* and *Medicina,* the polar tide seems to be "playing" against the instrumental trend. At the same time, the use of regression coefficients from the *EOST* website in calculations leads to better results, especially after additional removal of the pole tide from the difference series. The minimum RMSD value for the difference series after subtracting the atmospheric effect using the regression coefficients is observed for *Vienna* (0.695 μGal), the maximum - for *Medicina* (1.772 μGal).

Further Table 3 shows the RMSD values for the difference series obtained after subtracting the atmospheric gravimetric effect that was calculated in this work by spherical harmonic expansion of the surface atmospheric pressure of the *ERA5* project without taking into account the inverse barometer (see rows 6, 7). When shifting from *OBS–TH–Patm* series for the regression coefficient k_S (row 2) to the corresponding series of ours (row 6), the most pronounced decrease in the RMSD value of the residual series at *Medicina* and *Vienna* points - at the first point the RMSD decreases by 0.439 μGal to 1.115 μGal, in the second, by 0.097 μGal to 0.673 μGal. In this case, the calculation results "move away" from observations only at *Membach* point, where the RMSD value of the difference series increases by 0.332 μGal, reaching 1.716 μGal. Comparison of the *OBS–TH–Patm–PM* difference series obtained by additional subtraction of the pole tide leads to similar results. Again, the most significant drop in RMSD is observed at *Medicina* and *Vienna* points, where their values decrease by 0.343 (to 1.559) μGal and 0.295 (to 0.539) μGal, respectively. A noticeable gain from the introduction of PM correction is also noted at *Moxa* point (decrease in the RMSD value by 0.171 μGal to 0.784 μGal); the loss is again visible at *Membach* point (by 0.259 μGal to 1.550 μGal).

The situation is somewhat improved by the use of the inverse barometer effect, that is confirmed by the data for two difference series – *OBS–TH–Patm* and *OBS–TH–Patm–PM*. For the *OBS–TH–Patm* series (see rows 6 and 10), the most noticeable decrease in RMSD values is observed at *Medicina* and *Vienna* points, at the first one it was –0.086 μGal (up to 1.029 μGal), at the second - –0.065 μGal (up to 0.608 μGal). The smallest (by 0.029 μGal) discrepancy between the results of calculations and observations is still observed at *Membach* point.

After subtracting *PM* pole tide from the considered difference series (*OBS–TH–Patm–PM* series in rows 7 and 11), the RMSD values decreased most noticeably at *Medicina* (–0.156 μGal, to 1.403 μGal) and *Vienna* (–0.105 μGal, to 0.434 μGal). In addition to *Vienna* point, low (less than 1 μGal) RMSD values of the series under discussion were noted at *Moxa* (0.762 μGal) and *Strasbourg* (0.882 μGal) points.

Continuing the analysis of Table 3, we compare the results obtained with considered the inverse barometer effect by the authors of this article (rows 10, 11), and similar results published on the *EOST* website (rows 8, 9). Row 12 shows the discrepancies between the RMSD values for the difference series of two models, denoted as Δ1 (the variant of the difference series is indicated in brackets). It can be seen that for the *OBS–TH–Patm* series (rows 12), our

model is significantly (by 0.022 μGal) better than the *EOST* model only at *Vienna* point. After subtracting the pole tide for the *OBS–TH–Patm–PM* difference series (Δ2, row 13), the gain of our calculation at *Vienna* point reaches 0.048 μGal with the RMSD of residual series of 0.434 μGal.

At each of the six points of the *GGP* network considered in the work, the authors calculated the RMS deviation for the trends shown in Table 3 in rows 14 (calculations performed by the authors) and 15 (data published on the *EOST* website). To highlight the trends, we used a fifth-degree polynomial; in addition, harmonics with periods exceeding 60 days were taken into account. The most low-frequency trends were noted at *Membach* (RMSD is 1.405 μGal), *Bad Homburg* (RMSD is 1.356 μGal), and *Medicina* (RMSD is 1.359 μGal). The values of the RMS deviations of the corresponding series of trend components, representing the overwhelming part of the dispersion of the observation series at three named stations, are given in brackets. The lowest trend amplitude is observed at *Vienna*. The trend at *Membach* point is obviously instrumental in nature, which is indicated by the presence of five gaps in the annual series of observations in addition to the magnitude and nature of the trend.

In rows 16, 17 of Table 3 are given the RMSD values for the difference series after subtracting from the observed gravimetric series (*OBS*) the theoretical tide for the Earth with the ocean (*TH*), the atmospheric effect (*Patm*), calculated taking into account the inverse barometer effect, the pole tide (*PM*), which is mainly due to inaccuracies in the calculation of oceanic gravimetric effect and high-frequency noises, low-frequency trend (*TREND*) and residual tide in the range of periods up to 4 days (*TIDE*) together with the RMS deviation of the differences in these series (row 18). From the comparison of the indicated RMS deviations it follows that after removing the trends, our calculations (row 16) come nearest to the observational data than the calculations published on the *EOST* website (row 17). The only exception is *Membach*. The best results are still noted for *Vienna*, where the RMSD of the residual series obtained after subtracting the trend is 0.226 μGal, which is by 0.035 μGal less than the RMSD of the residual series determined from the results of the *EOST* calculations. For *Strasbourg* point, the advantage of our calculation reaches 0.032 μGal, for *Moxa* point - 0.019 μGal.

Thus, after removing the low-frequency trends (periods of more than 60 days), which, apparently, are mainly instrumental in nature, the results of our calculations of the atmospheric gravimetric effect begin to exceed the results of the *EOST*, since they turn out to be closer to the results of gravimetric observations. However, this conclusion is still preliminary - for final conclusions, an analysis of long-term series is required.

Software implementation of calculations. AURORA1.0_2019 program

The possibility of calculating the atmospheric gravimetric effect was implemented by us in the form of a computer program AURORA1.0_2019[1], which interface is shown in Fig. 4, *above*. To start the program, you need to enter the name of the station, its geographic coordinates, calendar dates of the beginning and end of the calculated interval, then press the RUN button.

In the head of the issuance protocol (see Fig. 4, *below*), in addition to the data entered by the user, the average value of the calculated series is given. The step of the outputted time

[1] Spiridonov E.A., Vinogradova O.Yu. The program AURORA1.0 for determining the atmospheric gravimetric correction for the operating systems WINDOWS 7, 8, 10. Certificate of state registration of the computer program No. 2019664579 of November 08, 2019.

series, which is the sum of the atmospheric loading effect and the atmospheric attraction, is 1 hour.

The input data for the program are not only the decomposition of the surface atmospheric pressure up to 360 order, obtained taking into account of the inverse barometer effect. To make corrections for the incompleteness of the decomposition, the initial pressure fields over the entire globe at mesh points 0.25×0.25° are also required. In this regard, the delivery of the program is possible only on external media with capacity of at least several terabytes. For remote users, the ATMOSPERIC GRAVITY website (http://volga19785.tmweb.ru) was created with the option to receive the calculation results on our e-mail address.

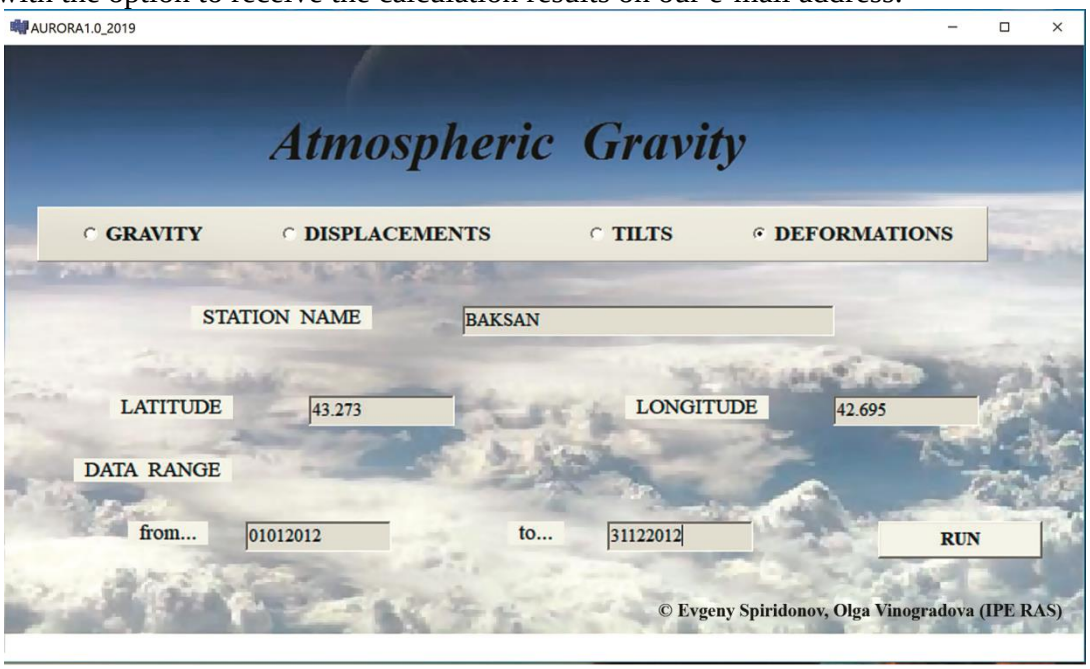

LEDOVO_ATMOSPERIC_GRAVITY_IB_2018_2019 — Блокнот

Файл Правка Формат Вид Справка

```
AURORA1.0_2019 (IPE RAS) 24/07/2019 13:13

ATMOSPERIC GRAVITY EFFECT
 (LOADING + ATTRACTION)

UNITS:      mcGal
STATION:    LEDOVO DOLGOYE
LATITUDE:   55.8578 deg
LONGITUDE: 37.9758 deg
MEAN:     -113.127  mcGal

21/06/2018 .... 19/04/2019  60 min

20180621000000  0.2824525
20180621010000  0.2261525
20180621020000  0.2825525
20180621030000  0.2713525
```

Fig. 4. Examples of the interface (*above*) and output protocol (*below*) of the AURORA1.0_2019 program for calculating the atmospheric gravimetric effect

Conclusions

The best results of calculating the atmospheric gravimetric effect that includes the atmospheric loading effect and the Newtonian direct attraction created by air masses, for six European points of the *GGP* network were obtained for *Vienna*. This point is equipped with a gravimeter that obtains the observations with the least instrumental trend, so that the pole tide is successfully measured. This circumstance explains the fact that the main conclusions of the work were formulated by the authors considering the data of *Vienna* point.

First of all, it should be noted that our results, obtained taking into account the effect of the inverse barometer, are in good agreement with the series presented on the *EOST* website. The RMSD of the difference series obtained by subtracting our results from the *EOST* results, according to observations for 2006 at different points, do not exceed 0.01–0.02 μGal.

The obtained results of calculating the atmospheric gravimetric effect after removing the low-frequency trend (periods exceeding 60 days) and high-frequency noises (periods up to 4 days) generally correspond better to the observational data than the series published on the *EOST* website - the maximum possible gain from the application of our method of the atmospheric effect calculation reaches 0.04 μGal.

Unremovable residuals in the range of periods from 4 to 60 days after subtracting the atmospheric effect reach 0.2–0.3 μGal and can be a consequence of, for example, hydrological or non-tidal oceanic effects. Reduction of these residuals is possible in the future through a more accurate calculation of the atmospheric effect.

The conclusions and estimates presented in the work are preliminary and will be specified by the authors in the future on substantially longer series.

At the time of the publication of this work (September, 2020), the results of calculating the atmospheric gravimetric effect (the sum of the atmospheric loading effect and the Newtonian direct attraction) for 2000–2019 are available on the Internet at our website Atmospheric Gravity (http://volga19785.tmweb.ru).

Acknowledgments

The work was carried out in accordance with the State assignment of Schmidt Institute of Physics of the Earth of the Russian Academy of Sciences.

References

Boy J.P., Chao B.F., Precise evaluation of atmospheric loading effects on Earth's time-variable gravity field, *J. Geophys. Res.*, 2005, vol. 110, B08412, doi: 10.1029/2002JB002333

Boy J.P., Gegout P., Hinderer J., Reduction of surface gravity data from global atmospheric pressure loading, *Geophys. J. Int.*, 2002, vol. 149, issue 2, pp. 534-545

Boy J.P., Hinderer J., Study of the seasonal gravity signal in superconducting gravimeter data, *Journal of Geodynamics*, 2006, vol. 41, pp. 227-233, doi: 10.1016/j.jog.2005.08.035

Dee D.P., Uppala S.M., Simmons A.J., Berrisford P., Poli P., Kobayashi S., Andrae U., Balmaseda M.A., Balsamo G., Bauer P., Bechtold P., Beljaars A.C.M., van de Berg L., Bidlot J., Bormann, N., Delsol C., Dragani R., Fuentes M., Geer A.J., Haimberger L., Healy S.B., Hersbach H., Hólm E.V., Isaksen L., Kållberg P., Köhler M., Matricardi M., McNally A.P., Monge-Sanz, B.M., Morcrette J.-J., Park B.-K., Peubey C., de Rosnay P., Tavolato C., Thépaut J.-N. and Vitart F., The ERA-Interim reanalysis: configuration and performance of the data assimilation system, *Q. J. R. Meteorol. Soc.*, 2011, vol. 137, pp. 553-597, doi: 10.1002/qj.828

Hinderer J., Crossley D., Scientific achievements from the first phase (1997–2003) of the Global Geodynamics Project using a worldwide network of superconducting gravimeters, *Journal of Geodynamics*, 2004. vol. 38, pp. 237-262.

Merriam J.B., Atmospheric pressure and gravity, *Geophys. J. Int.*, 1992, vol. 109, pp. 488-500.

Spiridonov E.A., Tidal Amplitude Delta Factors and Phase Shifts for an Oceanic Earth, *Izvestiya, Atmospheric and Oceanic Physics*, 2017, vol. 53, no. 8, pp. 813-846.

Spiridonov E.A., Atmospheric gravity effect, *Geophysical Research*, 2019, vol. 20, no. 3, pp. 45-70. (in Russian).
Spiridonov E.A., Vinogradova O.Yu., The Results of Integrated Modeling of the Oceanic Gravimetric Effect, *Seismic Instruments*, 2018, vol. 54, no. 1, pp. 43-53.
Spiridonov E.A., Yushkin V.D., Vinogradova O.Yu., Afanasyeva L.V., The Atlantida 3.1_2014 Program for Earth Tide Prediction: New Version, *Seismic Instruments*, 2018, vol. 54, no. 6, pp. 650-661.
Spratt R.S., Modelling the effect of atmospheric pressure variations on gravity, *Geophys. J. R. Astr. Soc.*, 1982, vol. 71, pp. 173-186.
Warburton R.J., Goodkind J.M., The influence of barometric pressure variations on gravity, *Geophys. J. R. Astr. Soc.*, 1977, vol. 48, pp. 281-292.